2022 44th Annual International Conference of
the IEEE Engineering in Medicine & Biology Society (EMBC)
Scottish Event Campus, Glasgow, UK, July 11-15, 2022

Broadband Microwave Electroporation Device for the Analysis of the Influence of Frequency, Temperature and Electrical Field Strength

Markus Paravicini[1], Manuela Milden[2], Laura M. Pimentel Paes Frank, Martin Schüßler[1], M. Cristina Cardoso[2], Rolf Jakoby[1] and Carolin Hessinger[1]

***Abstract*— In this paper, a broadband microwave device for cell poration is presented, that enables the analysis of the relation between frequency, electrical field strengths and temperature for a successful cell poration. Electromagnetic-thermal coupled simulations in the frequency range from 1 GHz to 10 GHz show that the device reaches electrical field strengths of 100 V/cm and temperatures lower then 40°C. Electroporation experiments with adherent C2C12 mouse myoblast cells show successful uptake of an anti-histone γ-H2A.X nanobody at a frequency of 10 GHz.**

***Clinical relevance*— This MWP device allows the fast electroporation of adherent cells. After 15 min, the cells show uptake of γ-H2A.X-specific nanobody while most of them survived.**

I. INTRODUCTION

Electroporation is a physical method to increase the cell membrane permeability in order to transport substances like DNA, nanobodies or peptides into the cell interior with the aim to modify its functionality or the cell itself [1]. Alternatives to a physical transfection are of biological or chemical nature. They enable a bypass of the cell membrane by modified viruses or chemicals. The major disadvantages of these methods are their limitations to the size and type of the substances to be transported, the limited usability for different cell lines and the toxicity of the chemicals. In contrast to this, electroporation is non-toxic and not limited to all types of substances or cell lines allowing the transfection of all types of biological substances [2]. These properties make it a proper candidate for many applications in biotechnology and medicine [3].

Classic electroporation devices are often container- or microfluidic-based systems, where the cells have to be in suspension during the procedure [4][5]. This means that the adherent cells have to be washed off from their seeding plate before electroporation, resulting in long waiting times till the cells adhere again and can be assayed. Furthermore, classical electroporation operates in a frequency range from kHz to MHz with high electrical field strengths up to $100\,000\,\frac{\mathrm{V}}{\mathrm{cm}}$ for successful electroporation [6]. These very high field strengths result in high cell death rates.

In contrast to this, microwave poration (MWP) devices operate in the GHz range. A successful electroporation was observed with significant lower electrical field strength of only $90\,\frac{\mathrm{V}}{\mathrm{cm}}$, resulting in a lower cell death rate [7]. Microwave induced electroporation devices were proposed with operating frequencies of $2.45\,\mathrm{GHz}$ and $18\,\mathrm{GHz}$ [7][8]. Up to now, the influence of the operating frequency on a successful electroporation is unclear. In this paper, a broadband device is proposed that enables a frequency depended analysis of the poration success of adherent cells. Moreover, the further relevant parameters that might influence the electroporation success could be analyzed that are electrical field strength and temperature [9][10].

First, the design and fabrication of the MWP device as well as the used cell line and dyes are described in section II. In section III, simulations were performed to match the design criteria. There, the results of the electrical field strengths and the reached temperatures are presented. To verify the simulation results, measurements of the S-parameters and the temperatures are performed in section IV. Further in this chapter experimental results of the microwave induced electroporation are shown. Finally, in V, a conclusion is drawn.

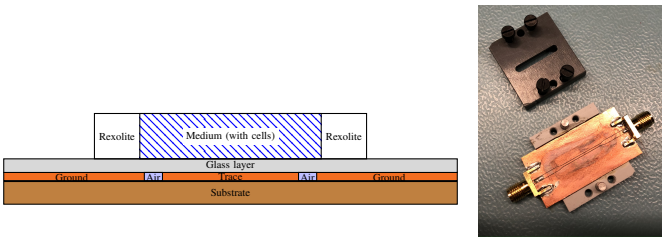

(a) (b)

Fig. 1: (a) Cross-section of the MWP device with Rexolite container and (b) 2-Port MWP device fabricated on Rogers RT/duroid 5880 with plastic cover.

II. MATERIALS & METHODS

A. MWP design & fabrication

The proposed MWP device was designed with Microwave Studio Suite from Dassault Systèmes to operate in a broad frequency range from $1\,\mathrm{GHz}$ to $10\,\mathrm{GHz}$ and has removable containers, where the cells can be seeded out. A cross section of this structure is shown in 1(a). Design objectives were to reach electrical field strengths larger than $100\,\frac{\mathrm{V}}{\mathrm{cm}}$ while the maximal temperatures of the material in the containers should stay below $40\,^{\circ}\mathrm{C}$ at power levels up to $0.5\,\mathrm{W}$. The

[1]Institute of Microwave Engineering and Photonics, Technical University of Darmstadt, 64283 Darmstadt, Germany markus.kochanek@tu-darmstadt.de

[2]Institute of Cell Biology and Epigenetics, Technical University of Darmstadt, 64287 Darmstadt, Germany

design is based on a tapered coplanar waveguide (CPW) (formed by the trace and grounds in Fig 1a), which is fabricated on a 787 µm Rogers RT/duroid 5880 substrate with a relative permittivity of $\varepsilon_r = 2.2 \pm 0.02$ and a loss tangent of $\tan(\delta) = 9 \cdot 10^{-4}$ at 10 GHz using photolithography. The substrate is coated with a copper layer with a thickness of 18 µm [11]. Removable containers glued on a thin glass substrate are proposed. The containers are fabricated out of Rexolite with a ground layer of low loss glass with a thickness of 100 µm, which is glued to the Rexolite container using a bio-compatible silicon glue [12][13][14]. Due to the removable containers the number of poration experiments per day can be increased while having a transparent container bottom allows the analysis of the porated cells using a microscope. To fix the position of the containers on the MWP device, a cover out of plastic is added. The cover includes a gap to position a thermocouple element. For transmission and reflection coefficient measurement, SMA connectors are soldered to the MWP device [15]. Fig. 1(b) shows the fabricated MWP device.

B. Cells & fluorescent dyes

Electroporation experiments are performed with C2C12 mouse cells. The C2C12 cell line is a subclone of myoblasts that were originally obtained by Yaffe and Saxel et al. [16]. C2C12 cells are cultured in DMEM 20% FCS growth medium in p60 plates at 37 °C in humidified atmosphere of 5% CO_2. One day before usage they were seeded into the gelatin-coated containers (in the 'water' area in 1a). Experiments are performed with 1000 - 5000 cells in total, which corresponds to a confluence of $20\% - 90\%$. On average, the cells were seeded with a confluence of 50%. Adherent C2C12 mouse cells were incubated with anti γ-H2A.X nanobody fused to the red fluorescent protein dTomato. The anti γ-H2A.X nanobody is a single-domain antibody fragment of camelids, which corresponds to the variable domain (VHH) of the heavy chain-only antibodies (HcAb) [17]. H2A.X is a phosphorylated form of the histone variant H2A.X modified at Ser-139. This modified form accumulates as a cellular response to DNA double strand breaks (DSB) [18]. DSBs arise from endogenous sources, such as collapsed replication forks, or can be caused by exogenous agents that include radiation, reactive oxygen species, and chemotherapeutic drugs such as topoisomerase II poisons [19]. For inducing DSB, UVC irradiation (crosslinker UVC500-230V from Pharmacia Biotech) 20 s, $12 \cdot 100 \frac{\mu J}{cm^2}$ are used. The nanobody was added right before the microwave exposure and removed immediately afterwards by washing with PBS and adding fresh growth medium. Untreated controls with and without crosslinking were preformed in parallel. The nanobody uptake into the cells is independent on DNA damage and as such, it reports on positive electroporation. As any other antibody/nanobody it reports on the ability to cross the cellular membrane into the cell's interior.

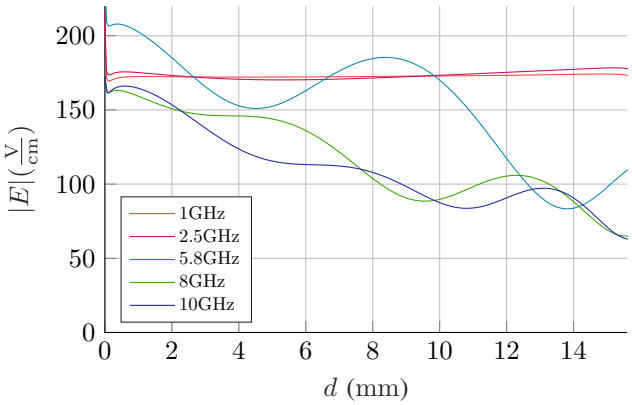

Fig. 2: Electrical field strength inside the medium (water) in the container for a frequency range from 1 GHz to 10 GHz at 0.5 W.

III. SIMULATIONS

A. MWP simulations

Electromagnetic (EM) simulations of the MWP device loaded with a container filled with water (based on a Debye model) are performed to analyze the electrical field strength along the transmission line. The input power to achieve those electrical field strengths is limited due to the temperature constraint. Temperatures must not succeed 40 °C to ensure the viability of the cells. Therefore, temperature and electrical field strength simulations are performed to obtain a geometry that meets the requirements in a frequency range from 1 GHz to 10 GHz.

1) Electrical field strength: According to the work from Schmidt et al. [7], microwave induced electroporation was observed at an operating frequency of 18 GHz for electrical field strengths above $100 \frac{V}{cm}$. In this work, the broadband MWP device is designed in a way that the threshold of $100 \frac{V}{cm}$ is exceeded for the frequency range from 1 GHz to 10 GHz. Fig. 2 shows the simulation results of the electrical field strengths along the gap that is loaded with the container construction for frequencies between 1 GHz to 10 GHz for an input power of 0.5 W. The electrical field strength decreases along the propagation direction and with frequency. After 8 mm - 9 mm the electrical field strength for 8 GHz and 10 GHz are lower then $100 \frac{V}{cm}$. At frequencies of 1 GHz and 2.5 GHz, the electrical field are nearly constant along the length of the whole distance of the container.

2) Temperature: In order to simulate the temperatures during the electroporation, thermal simulations based on the calculated losses of the EM simulation are performed with the thermal solver of CST. The ambient temperature selected for the simulations is equal to the ambient temperature of the lab and equals 22 °C. The temperature is analyzed for a frequency range from 1 GHz to 10 GHz using power levels of up to 0.5 W. For all analyzed frequencies and power levels the temperature is < 40 °C, guaranteeing that the cells are not killed by hyperthermia. Fig. 3 shows the temperature distribution within the container along the transmission line

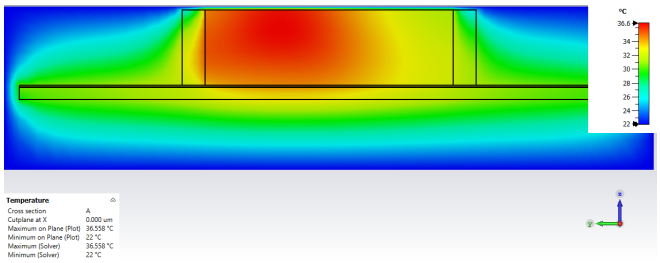

Fig. 3: Temperature distribution for 10 GHz at a power level of 0.5 W in steady-state case.

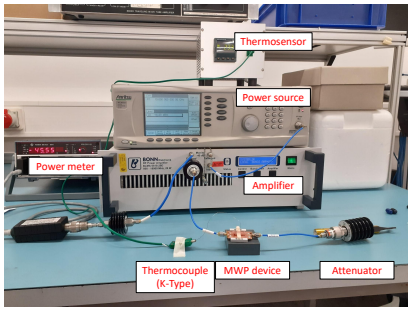

Fig. 4: The measurement setup with a thermo sensor, a power source, an amplifier and the MWP device.

in the steady-state case for 10 GHz at a power level of 0.5 W.

IV. MEASUREMENTS

The measurement setup for the experimental validation includes a signal generator (Anritsu MG3692A) and an amplifier (BLMA 0818-30/20D from BONN Elektronik) to amplify the MW signal as shown in Fig. 4. MWP experiments are performed in the frequency range from 1 GHz to 10 GHz with power levels of 28 dBm to 32 dBm. To monitor the temperature during the poration process, a thermocouple element is inserted into the sample container. To monitor the power level of the amplified signal, a power meter is used, which guarantees that the desired power level is applied to the MWP device.

A. Comparison of simulation and measurement results

The simulated and measured reflection and transmission coefficient $|S_{11}|$ and $|S_{21}|$ are shown in Fig. 5. Over the whole operation frequency range, the measured transmission coefficient $|S_{21}|$ of the MWP device is in good agreement to the simulations. For higher frequencies, the differences between the simulated and measured values increase, but still with the same course. The differences between the measured and simulated $|S_{11}|$ are larger compared to the differences of the simulated and measured $|S_{21}|$, especially in the frequency range from 0.5 GHz to 3 GHz and from 8.5 GHz to 10 GHz. These differences can be explained by the influence of the position of the container and the soldering of the SMA connector.

For temperature measurements, the thermocouple element is inserted at the same position where the temperature is extracted in the simulation model. Temperature measurements

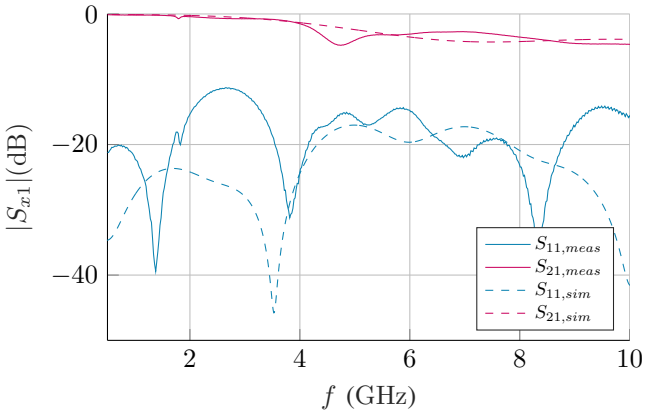

Fig. 5: Simulated and measured $|S_{11}|$ and $|S_{21}|$ parameters from the MWP device in a frequency range from 1 GHz to 10 GHz.

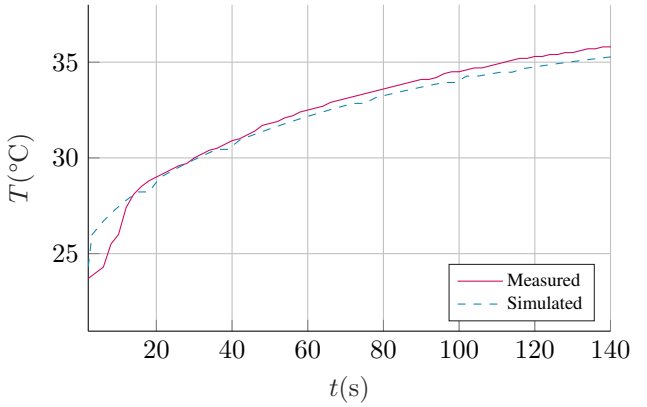

Fig. 6: Simulated and measured temperature over time at a frequency of 10 GHz at 0.5 W.

are performed at a power level of 0.5 W. Fig. 6 shows the temperature profile for simulated and measured data. The simulated and measured temperature profiles fits good to each other.

In the next step, electroporation experiments are performed in the bio lab to show the functionality of the proposed device.

B. Electroporation

Within the operation frequency range between 1 GHz-10 GHz, two distinct frequencies at 5.8 GHz and 10 GHz were selected to prove the concept of an successful microwave-induced electroporation. The experiments were performed with varying durations (10 min to 20 min) and input powers (0.3 W to 0.7 W). At the operation frequency of 10 GHz and power levels of 0.4 W to 0.7 W, the experiments show promising results regarding the uptake rate and viability of the cells. In Fig. 7, uptake of the anti-γ-H2A.X nanobody in C2C12 cells are shown, while no uptake of the anti-γ-H2A.X nanobody in the untreated control group is shown in Fig. 8. The measured temperature of the medium inside the

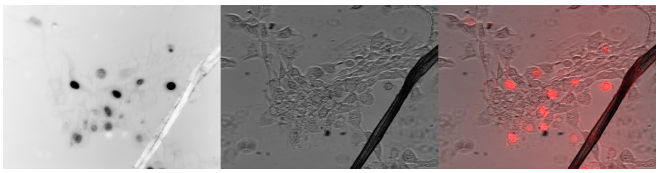

Fig. 7: Uptake of the anti-γ-H2A.X nanobody (red labeled) in adherent C2C12 cells after microwave-induced electroporation at $10\,\mathrm{GHz}$ and $0.7\,\mathrm{W}$ for $15\,\mathrm{min}$. The left image shows red fluorescence of the nanobody, the image in the middle depicts the cells in phase contrast and the right image is an overlay of both.

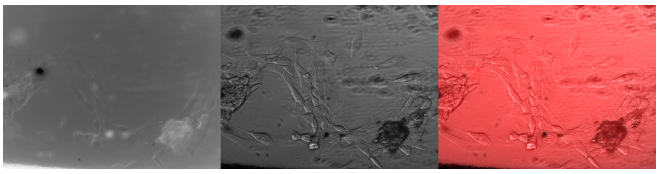

Fig. 8: No uptake of the anti-γ-H2A.X in adherent C2C12 cells without microwave-induced electroporation. The left image shows red fluorescence of the nanobody, the image in the middle depicts the cells in phase contrast and the right image is an overlay of both.

container is always $\leq 38\,^{\circ}\mathrm{C}$ during the experiments. Due to this, the uptake of anti-γ-H2A.X nanobody into the cells due to hyperthermia can be excluded.

V. CONCLUSIONS

In this paper, a MWP device was presented, which allows the analysis of the influence of the three main parameters of microwave induced electroporation: Frequency, temperature and electrical field strength. It has been shown in simulations and measurements, that the MWP design is broadband and reaches the design targets of an electrical field strengths of $> 100\,\frac{\mathrm{V}}{\mathrm{cm}}$, while not exceeding a temperature of $40\,^{\circ}\mathrm{C}$ at the bottom of the container, where the adherent C2C12 myoblast mouse cells are located. MWP experiments with adherent C2C12 mouse cells and anti-γ-H2A.X nanobody showed, that electroporation occurs at $10\,\mathrm{GHz}$. Based on this promising results, the next step will be a comprehensive analysis with the proposed broadband MWP device, using additional frequencies and power levels in order to find a mathematical relationship that describes the interaction and influences of the relevant poration parameters for a successful electroporation. Furthermore, experiments with more cell lines will be performed to validate and extend the model.

ACKNOWLEDGMENT

The authors acknowledge support by the German Research Foundation project number 'JA 921/73-1' and 'CA 198/17-1'. We are indebted to Etienne Weiss (CNRS - Université de Strasbourg, France) for the gift of the anti-γ-H2A.X nanobody construct.

REFERENCES

[1] U. Rothbauer *et al.*, "Targeting and tracing antigens in live cells with fluorescent nanobodies," *Nature methods*, vol. 3, no. 11, pp. 887–889, 2006.
[2] T. K. Kim and J. H. Eberwine, "Mammalian cell transfection: the present and the future," *Analytical and bioanalytical chemistry*, vol. 397, no. 8, pp. 3173–3178, 2010.
[3] T. Kotnik, *et al.*, "Electroporation-based applications in biotechnology," *Trends in biotechnology*, vol. 33, no. 8, pp. 480–488, 2015.
[4] Y. S. Shin, K. Cho, J. K. Kim, S. H. Lim, C. H. Park, K. B. Lee, Y. Park, C. Chung, D.-C. Han, and J. K. Chang, "Electrotransfection of mammalian cells using microchannel-type electroporation chip," *Analytical chemistry*, vol. 76, no. 23, pp. 7045–7052, 2004.
[5] A.-Y. Chang, X. Liu, H. Tian, L. Hua, Z. Yang, and S. Wang, "Microfluidic electroporation coupling pulses of nanoseconds and milliseconds to facilitate rapid uptake and enhanced expression of dna in cell therapy," *Scientific reports*, vol. 10, no. 1, pp. 1–10, 2020.
[6] J. C. Weaver, K. C. Smith, A. T. Esser, R. S. Son, and T. Gowrishankar, "A brief overview of electroporation pulse strength–duration space: A region where additional intracellular effects are expected," *Bioelectrochemistry*, vol. 87, pp. 236–243, 2012.
[7] S. Schmidt *et al.*, "Microwave induced electroporation of adherent mammalian cells at 18 ghz," *IEEE Access*, vol. 7, pp. 78 698–78 705, 2019.
[8] E. K. Ahortor, D. Malyshev, C. F. Williams, H. Choi, J. Lees, A. Porch, and L. Baillie, "The biological effect of 2.45 ghz microwaves on the viability and permeability of bacterial and yeast cells," *Journal of Applied Physics*, vol. 127, no. 20, p. 204902, 2020.
[9] S. Atmaca, Z. Akdag, S. Dasdag, and S. Celik, "Effect of microwaves on survival of some bacterial strains." *Acta microbiologica et immunologica Hungarica*, vol. 43, no. 4, pp. 371–378, 1996.
[10] S. Banik, S. Bandyopadhyay, and S. Ganguly, "Bioeffects of microwave—-a brief review," *Bioresource technology*, vol. 87, no. 2, pp. 155–159, 2003.
[11] *RT/duroid 5870/5880 High Frequency Laminates*, Rogers Corporation, 2017, rev. 1306 060117.
[12] *Product: Rexolite 1422 (Cross Linked Polystyrene)*, C-Lec Plastics Inc., 2015.
[13] *AF32 eco Thin Glass*, Schott AG, thickness: 200µm.
[14] *SCRINTEC 901*, Scrint, 2018.
[15] *Square flange jack receptacle with shoulder contact*, Radiall, partNum: R125512000.
[16] D. Yaffe and O. Saxel, "Serial passaging and differentiation of myogenic cells isolated from dystrophic mouse muscle," *Nature*, vol. 270, no. 5639, pp. 725–727, 1977.
[17] E. Moeglin, D. Desplancq, A. Stoessel, C. Massute, J. Ranniger, A. G. McEwen, G. Zeder-Lutz, M. Oulad-Abdelghani, M. Chiper, P. Lafaye *et al.*, "A novel nanobody precisely visualizes phosphorylated histone h2ax in living cancer cells under drug-induced replication stress," *Cancers*, vol. 13, no. 13, p. 3317, 2021.
[18] L. Mah, A. El-Osta, and T. Karagiannis, "γh2ax: a sensitive molecular marker of dna damage and repair," *Leukemia*, vol. 24, no. 4, pp. 679–686, 2010.
[19] A. Ciccia and S. J. Elledge, "The dna damage response: making it safe to play with knives," *Molecular cell*, vol. 40, no. 2, pp. 179–204, 2010.